Photoionization yields in the doubly doped SrF_2:Eu,Sm system

Robert L. Fuller and Donald S. McClure
Frick Chemical Laboratory, Princeton University, Princeton, New Jersey 08544
(Received 5 July 1990)

The doubly doped SrF_2:Eu,Sm system was examined as a model system for the photoionization process. These crystals were codoped with 0.01 mol % Eu^{2+} and 0.02 mol % Sm^{3+}. From optical-absorption measurements, the absolute ionization efficiency of Eu^{2+} was found to be 0.65% at 295 K and 1.6% at 310 K upon irradiation with 4.9-eV light in this system. The $Sm^{3+}\cdot F^-$ centers were found to be the principal traps for the generated electrons. The temperature dependence of the ionization efficiency of Eu^{2+} with irradiation at 5.2 and 5.7 eV led to the measurement of an activation barrier of 0.34 eV. These experiments also show that only cubic Eu^{3+} is initially formed upon photoionization of Eu^{2+} and that subsequently an interstitial fluoride-ion charge compensates the Eu^{3+} ion. The photoconductivity does not show a temperature dependence corresponding to that of the ionization yield. This result leads us to propose that the trapping of electrons at the majority $Sm^{3+}\cdot F^-$ sites is followed by a reverse F_i^- current from trap to donor, which cancels the electron current. The measured photocurrent arises from the small minority of other traps present. A mechanism is proposed to explain the observed yields and temperature dependence.

I. INTRODUCTION

Several divalent rare-earth-doped alkaline earth fluorides have been studied as model systems of the photonization process in ionic crystals, and some information has been obtained regarding these systems's photoionization thresholds[1,2] and their rates of photoionization.[3,4] This paper presents information on the absolute ionization efficiency of Eu^{2+} in the SrF_2 host and the relative ionization efficiency of SrF_2:Eu^{2+} as a function of temperature. To our knowledge, there has never been a measurement of the ionization efficiency of an impurity in an ionic crystal, so these results are of importance in understanding the ionization process in these kinds of systems.

Feofilov, and later Welber reported the following reversible photoreaction in CaF_2:[5]

$$Eu^{2+}+Sm^{3+}\rightleftarrows Eu^{3+}+Sm^{2+}\ . \tag{1}$$

By irradiating with either 4.9-eV (254-nm) light or 3.9-eV (313-nm) light, the forward reaction or the backward reaction was observed, respectively. Photoconductivity measurements (to be presented) show that a divalent impurity, either Eu^{2+} for 4.9-eV light or Sm^{2+} for 3.9-eV light, absorbs the appropriate photon and photoionizes and ejects an electron into the conduction band. Subsequently, a trivalent impurity, either Eu^{3+} or Sm^{3+}, will act as a trap and capture the free conduction-band electron, thus forming the corresponding divalent impurity. This overall process depends on many factors: the absorption coefficient of both divalent impurities at a given wavelength of light, the photoionization efficiency of both divalent impurities at that wavelength, the concentration of each type of trivalent impurity trap, and the capture cross section of each type of trivalent trap.

All of the quantities which affect this reaction are of interest when forming and testing photoconductivity models; and the experiments involving the doubly doped SrF_2:Eu,Sm system can answer some questions concerning the photoionization process. Also, systems such as MgS:Eu,Sm and BaFBr:Eu^{2+} are of interest for storage phosphors, and this work may provide insight into these types of systems.[6,7] In Welber's study, either the 4.9-eV (254-nm) or the 3.9-eV (313-nm) mercury line excited his doubly doped CaF_2:Eu,Sm crystal while only the CaF_2:Sm^{2+} fluorescence at 14 100 cm^{-1} was monitored. This configuration verified the overall electron-transfer reaction; however, since monitoring fluorescence determines only *relative* changes in the Sm^{2+} concentration, an *absolute* efficiency of Sm^{2+} formation was not determined. The efficiency of Sm^{2+} formation is related to the efficiency of Eu^{2+} ionization because, if every photoionized electron originates only from a Eu^{2+} and is captured only by a Sm^{3+} trap, then efficiency of Sm^{2+} formation is a direct measurement of the photoionization efficiency of Eu^{2+}. We have measured the photon flux incident on our SrF_2:Eu,Sm crystals, determined the absolute concentrations of the divalent impurities from room-temperature absorption spectra, and calculated the photoionization efficiency of Eu^{2+} in SrF_2 at 4.9 eV to be 0.65% at 295 K and 1.6% at 310 K. These results are presented in detail in Sec. III B.

The doubling of the ionization efficiency of Eu^{2+} upon changing the temperature from 295 to 310 K implies that temperature has a strong effect on photoionization yield. To investigate this phenomenon further, a temperature study of the ionization efficiency in the SrF_2:Eu,Sm doubly doped system was performed. In Sec. III D, it is proved that, after a divalent europium ionizes, a cubic (uncompensated) Eu^{3+} ion is formed. At room temperature, the $Eu^{3+}(O_h)$ eventually becomes compensated

with an interstitial fluorine ion (F_i^-). Cooling of the sample below 300 K significantly reduces the movements of the interstitial fluorines. By using the fluorine motion to our advantage, the efficiency of Eu^{3+} formation as a function of temperature could be obtained using excitation spectroscopy, and is presented in Sec. III E.

II. EXPERIMENTAL

The doubly doped samples were all cut from a boule of SrF_2 doped with nominal concentrations of 0.01 mol % europium and 0.02 mol % samarium. The absorption of the boule was checked to see if any concentration gradients existed in the boule (one of our CaF_2:Eu,Sm boules did show a concentration gradient of Eu^{2+} and Sm^{2+}). However, no gradients were observed in the SrF_2:Eu,Sm boule. The SrF_2:0.02% Sm^{2+} standard sample was prepared using additive coloration techniques.[8,9] All samples were purchased from Optovac.[10]

Our photoconductivity measurements were done using a blocking-electrode configuration.[11] The electrodes were fine Ni mesh which were sandwiched between two dielectric plates made of quartz. The front electrode is charged to a value near -500 V. The back electrode was in series with a grounded 10^{12}-Ω resistor; the voltage across this resistor was measured with a vibrating reed electrometer, Cary Model 401. Typical signals were $\sim 10^{-13}$ A. A Hanovia 2000-W xenon lamp was focused into a Jobin-Yvon H20 single monochromator which selected the proper wavelength of light for irradiation. The 2-mm slits of the monochrometer provided a spectral resolution of 8 nm. Light exiting the monochrometer was subsequently filtered to remove short wavelengths of light since the photocurrents from these wavelengths can be orders of magnitude higher per absorbed photon than the photocurrents near the photoionization thresholds. Typical photon densities were $\sim 10^{13}$ photons/s on the sample area of ~ 0.2 cm^2.

In the absolute efficiency experiments, a 200-W mercury lamp and a 10-nm bandwidth 254-nm (4.9-eV) interference filter were used to select the ionizing light. A cardboard mask with the same dimensions as the crystal held the crystal during the irradiation period. For the setup of sample 1, the cardboard mask was directly behind the interference filter, which effectively raised the temperature of the sample to 310 K, as measured by a thermocouple. In the setup of sample 2, the mask was thermally isolated from the hot interference filter so the sample was maintained at room temperature, 295 K. Once the sample had been irradiated, it was removed from the mask and an actinometer cuvette was placed directly behind the mask to calibrate the lamp. A $K_3Fe(C_2O_4)_3$ actinometer solution, which has been shown to be quite accurate in the ultraviolet region of the spectrum, was used.[12,13] We followed the recommended procedure in Ref. 13 with a control cuvette to monitor any stray light. The entire irradiation configuration was placed in a dark room so the amount of stray light was minimal. A diode array spectrometer measured the actinometer intensity in less than 10 s again to avoid stray light. Reflection corrections for the quartz cuvette in the actinometer measurements were assumed to be equivalent to the reflection losses found at the sample, therefore no correction was made. For sample 1, the actinometer results showed that $(6.33\pm0.13)\times10^{15}$ photons/min were incident on the sample's area of 36.3 mm^2. When calculating the absorbed photons by the sample this average value was used. Because a new lamp was used in the measurements of sample 2, the actinometer results increased from (5.8 to 7.0)$\times10^{15}$ photons/min incident on sample 2 having an area of 39.1 mm^2. When calculating the absorbed photons for this sample, the actinometer measurements which were taken directly after each irradiation period were used. Sample 1 was 2.40 mm thick and sample 2 was 2.15 mm thick.

The absorption measurements of the SrF_2:Eu,Sm samples were performed on a Cary 14 spectrometer. A special sample holder was used to hold and mask the samples in the spectrometer, and a matching mask was placed in the reference light path. This sample holder allowed samples to be located at the identical position in the light path from day to day. The baselines were obtained by using a 2.4-mm thick undoped SrF_2 crystal from Harshaw.

For the relative efficiency experiments, a more powerful light source than a mercury lamp was needed. Using a β-barium borate (BBO) crystal, the second harmonic of a YAG:Nd^{3+} laser was converted into the fourth harmonic at 266 nm (4.6 eV).[14] However, this wavelength is poorly absorbed by the doubly doped crystal [D_O (optical density)≈ -0.1], so the 266-nm (4.6-eV) laser beam of ~ 50 mJ per pulse was focused into a hydrogen Raman cell to generate the first and second anti-Stokes shift at 5.2 eV and 5.7 eV, respectively. Both of these wavelengths are strongly absorbed by the doubly doped samples (all of which had $D_O > 1.5$, thus absorbing $>97\%$ of the light). Typical ionizing pulse energies were ~ 1 mJ and were focused to a ~ 2-mm spot. The samples were approximately cubes with 3 mm per side and were mounted in a coldfinger. For every measurement, a new sample was used. The samples were cooled to a specific temperature by using a solvent–liquid-nitrogen mixture in the coldfinger; the exact temperature was defined by the solvent's freezing point.[15] This technique provided stable temperatures for the samples while they were being irradiated with the ionizing radiation. A thermocouple surrounded by indium metal was placed between the sample and the cold block in order to measure the temperature of the sample.

After photoionization, the relative number of trivalent impurities was measured using excitation spectroscopy. Both Eu^{3+} and Sm^{3+} absorb at $\sim 19\,000$ cm^{-1} and fluoresce at $\sim 17\,900$ cm^{-1} (see Sec. III C); this situation permitted a comparative excitation experiment to be performed. A nitrogen laser-pumped dye laser system from Molectron provided tunable laser light for the experiment. The fluorescence was collected at right angles and was focused into a Jobin-Yvon H20 single monochromator set at 560 nm (17 900 cm^{-1}) with 4-nm resolution and a 1P28 photomultiplier tube. To ensure that we sampled the region of the crystal that had been irradiated with the ionizing light (at 5.2 or 5.7 eV), two irises defined an axis which was accurate to within a few degrees; both the ion-

izing light and the tunable dye light followed this axis. Wavelength calibrations were performed for one SrF_2:0.01% Eu,0.02% Sm sample using several neon optogalvanic transitions and an etalon and are accurate to 1 cm^{-1}.[16] Figures 5–7 have been drawn with a linear wave-number scale and uncorrected spectra so that exact spectral line positions cannot be inferred from them, but correct values are quoted in the text.

Because these excitation experiments were relative measurements, a reference was needed to calculate the number of cubic Eu^{3+} atoms formed. A convenient solution to the problem was to ionize the sample at 295 K where the ionization efficiency of Eu^{2+} was known to be 0.65%; hence, the efficiency of Eu^{3+} formation is also 0.65%. By annealing the sample at that temperature until all the newly formed Eu^{3+} was fluorine compensated, the intensity of the $Eu^{3+}\cdot F^-(C_{4v})$ band was proportional to the number of Eu^{3+} ions formed. Subsequent ionization at lower temperatures resulted in only cubic Eu^{3+} being formed. The intensity of the $Eu^{3+}(O_h)$ band could be directly compared to the intensity of the $Eu^{3+}\cdot F^-(C_{4v})$ band previously formed, and a relative efficiency of Eu^{3+} formation at that temperature could be determined.

III. RESULTS

A. Photoconductivity spectra

In the Introduction, it was suggested that the mechanism of the electron-transfer reaction shown in Eq. (1) is achieved through the photoionization of the divalent impurities. This notion is confirmed by the photoconductivity spectra of the doubly doped SrF_2:Eu,Sm system which is shown in Fig. 1 for two states ("states" denotes the condition of a crystal after a period of irradiation at 4.9 eV). Since this technique directly measures the free electrons in the SrF_2 conduction band, these spectra prove that the divalent impurities are photoionizing. The spectrum of SrF_2:Eu,Sm sample in the "initial" state is identical to the photoconductivity spectrum of single doped $SrF_2:Eu^{2+}$, with the exception of a weak tail at 32 000 cm^{-1} (4.0 eV), suggesting that the majority of photoionizing centers in the initial state are divalent europium.[2] The tail is attributed to a small amount of divalent samarium which is also present in the sample. This interpretation of the unirradiated "initial" state is supported by the absorption spectrum of this sample, which shows that the europium in this sample is divalent, and the majority of the samarium is trivalent. After irradiation of the sample at 4.9 eV, the spectrum of the "green" state in Fig. 1 was recorded (the presence of Sm^{2+} colors the samples green). The weak tail at 32 000 cm^{-1} from the initial state has grown to a distinct peak with a maximum at 34 000 cm^{-1}, which corresponds to a maximum in the $SrF_2:Sm^{2+}$ absorption spectrum. Also, the initial strong Eu^{2+} signal has, correspondingly, decreased. These observations simply reflect the charge-transfer reaction between europium and samarium depicted in Eq. (1). Because the Sm^{2+} ion apparently ionizes at lower energies than the Eu^{2+} ion, the photoionization threshold for $SrF_2:Sm^{2+}$ can be determined from this spectrum and is estimated to occur at 3.4 eV (27 000 cm^{-1}).

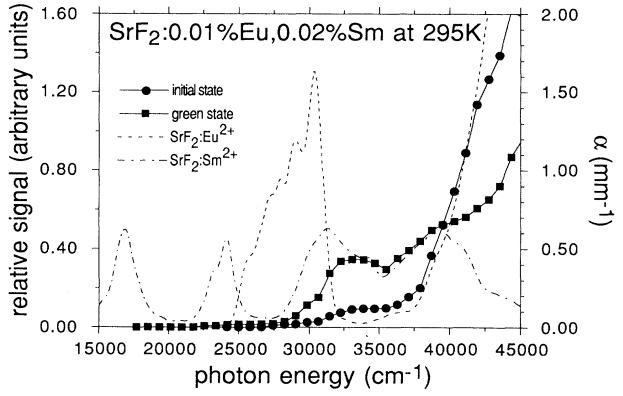

FIG. 1. Photoconductivity spectra of the doubly doped SrF_2:Eu,Sm sample at 295 K. The spectrum of the initial sample is similar to the spectrum of singly doped $SrF_2:Eu^{2+}$, with the exception of a tail at 32 000 cm^{-1} (4.0 eV). This tail is attributed to a small amount of divalent samarium which is also present in the sample. After irradiation at 4.9 eV (39 000 cm^{-1}), the second spectrum (the green state) was recorded. The small tail at 32 000 cm^{-1} has grown to a full sized peak with a maximum at 34 000 cm^{-1}, which corresponds to a maximum in the $SrF_2:Sm^{2+}$ absorption spectrum. The absorption spectra of SrF_2:0.02% Eu^{2+} and SrF_2:0.02% Sm^{2+} are shown for comparison by the broken lines.

The photoconductivity spectrum for the doubly doped SrF_2:Eu,Sm sample at 80 K is shown in Fig. 2. Because the samples become polarized by the ionizing light, the absolute magnitude of the photocurrent has a relatively large uncertainty; however, each photoconductivity spectrum is very reproducible. The samples were depolarized after each spectrum, and this technique gave absolute magnitudes within a factor of 4. Note that the magnitude of the photoconductivity spectra taken at 295 K (Fig. 1) are within the factor of 4 to those taken at 80 K. The spectra of the two states in Fig. 2 are similar to the ones shown in Fig. 1.

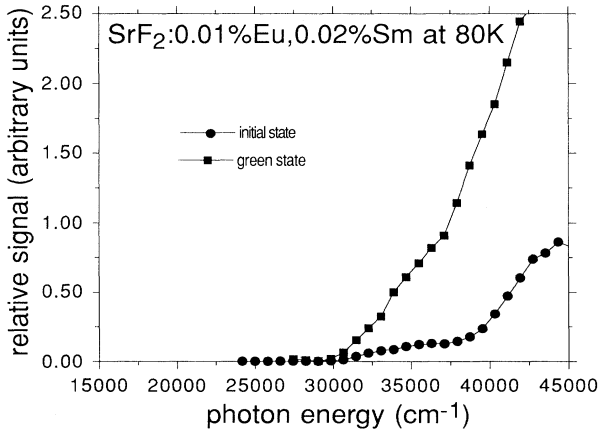

FIG. 2. Photoconductivity spectra of the doubly doped SrF_2:Eu,Sm sample at 80 K. The absolute magnitudes of the signals are difficult to reproduce accurately, but the currents change at most by a factor of 4 between 80 and 295 K.

B. Absolute ionization efficiencies—absorption spectra

Our principal goal was to measure quantitatively the charge transfer between europium and samarium and to use these results in forming and evaluating models for the photoionization process. The photoconductivity technique could be used to monitor the reaction; however, because of small signals and polarization of samples (formation of microscopic concentration gradients of the impurities due to the application of fields), a simpler way to monitor the reaction was to measure changes in the optical absorption of the Eu^{2+} and Sm^{2+} after periods of irradiation. The divalent rare earths all have strongly allowed $f \rightarrow d$ transitions;[17–19] therefore, this technique should be quite sensitive. The absorption spectra of one of our SrF_2Eu,Sm samples in two states is shown in Fig. 3. These spectra are simply a composite of the separate spectra of SrF_2:Eu^{2+} and the SrF_2:Sm^{2+}. One can clearly see that the large band at 30 400 cm^{-1}, due to the Eu^{2+} impurity, shrinks as the crystal is irradiated with the 4.9-eV light, while the small band at 16 900 cm^{-1}, due to the Sm^{2+} impurity, grows. Since Eu^{2+} is the only species absorbing initially at 4.9 eV, a fraction of such photons will produce Eu^{3+} and an electron: Since Sm^{3+} is the only trivalent trap ion present in significant amounts, one Sm^{2+} should be produced for each electron trapped. Thus, the decrease in the numbers of Eu^{2+} ions should equal the increase in the numbers of Sm^{2+} ions for the initial period of irradiation. The experiments described in the following show that this is true.

It is necessary to know at least the relative values of the absorption coefficients of Eu^{2+} and Sm^{2+} in order to prove that each Eu^{2+} ionized leads to one Sm^{2+}. An absolute value was determined by reducing a SrF_2:0.02% Sm^{3+} crystal to Sm^{2+}, a procedure used by Kaiser, Garrett, and Wood.[20] In this way, we found $K = 7.8$ cm^{-1} for the 16 900 cm^{-1} band at 295 K (corrected to 0.01 mol %). Arkhangel'skaya, Kiselyeva, and Shraiber found the absorption coefficient of the corresponding band in the CaF_2:Sm^{2+}, at 16 100 cm^{-1} to be $K = 9.3$ cm^{-1} at 300 K and 0.01 mol %.[21] The close correspondence of these two values supports our result for SrF_2:Sm^{2+}. We next used this spectrum of SrF_2:0.02 %Sm^{2+} to fit the spectrum of doubly doped samples in the region of 16 900 cm^{-1} and thereby determined the concentration of Sm^{2+} in these samples.

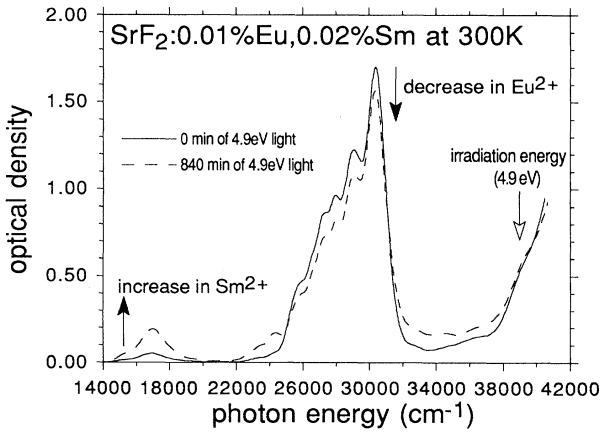

FIG. 3. Two absorption spectra of SrF_2:0.01 % Eu,0.02% Sm recorded at 295 K before and after 4.9-eV irradiation at 295 K. These spectra are simply composites of the singly doped one-photon spectra of Eu^{2+} and Sm^{2+} doped into SrF_2 shown in Fig. 1. The band at 17 000 cm^{-1} permits a quantitative calculation of the amount of Sm^{2+} in the crystal. These spectra were from sample 1.

The absorption coefficient of SrF_2:Eu^{2+} at the absorption maximum at 30 400 cm^{-1} could be determined from the decrease in Eu^{2+} and the increase in Sm^{2+} in the SrF_2:Eu,Sm samples if we assumed that every Eu^{2+} lost corresponded to one Sm^{2+} formed. The value would be $K = 16.3$ cm^{-1} at 295 K and 0.01 mol % if this were true. Again, we compared our result to that of Arkhangel'skaya for CaF_2:Eu^{2+}, who found $K = 17.9$ cm^{-1} at 300 K and 0.01 mol %. The close agreement of these two numbers supports the hypothesis that each Eu^{2+} ionized leads to formation of one Sm^{2+}. To further corroborate this, we checked the absorption coefficient for a sample of SrF_2:0.02% Eu^{2+} (in this sample, the ratio of Eu^{3+} to Eu^{2+} was determined to be less than 1:1000 using the excitation technique in Sec. III C). The absorption coefficient determined from this sample agreed with that determined from the doubly doped sample. This result also shows that the number of other electron traps in the crystal is small compared to the number of Sm^{3+} traps.

The number of 4.9-eV photons absorbed by the sample was determined by actinometry performed on the irradiated area, as described earlier, and from the optical density of the sample. From a comparison of the spectra of SrF_2:0.02% Eu^{2+} and SrF_2:0.02% Sm^{2+} to the spectrum of the sample, the fraction of the optical density due to Eu^{2+} and Sm^{2+} at 4.9 eV was calculated; the fraction of the optical density due to Eu^{2+} was always greater than 80% of the total optical density. The total optical density was never greater than 0.6, so the photon density did not change significantly throughout the thickness of the crystal. By measuring either the decrease in the Eu^{2+} peak or the increase in the Sm^{2+} peak, the quantum yield of the ionization reaction over a time interval was measured. The Sm^{2+} peak was spectrally isolated from the Eu^{2+} bands (the reverse is not so); and these data were the more accurate.

Figure 4 shows that Sm^{2+} production varies linearly with the number of absorbed photons at early times. We inadvertently made these measurements at two different temperatures, and from the slopes found an ionization efficiency for Eu^{2+} (Φ_{Eu}) of 0.65±0.10 % at 295 K and 1.6±0.2 % at 310 K for SrF_2:0.01% Eu,0.02% Sm. The errors were calculated assuming a systematic error from the irradiating lamp which accumulates with each irradiation period and a random error from errors in the measurement and fit of the Sm^{2+} band. We used the standard deviation of the two fits in Fig. 4 as a measurement of the random error. These figures show that there is a strong temperature dependence in the ionization yield; this dependence was confirmed by making relative yield measurements over a much wider temperature range (Sec. III E).

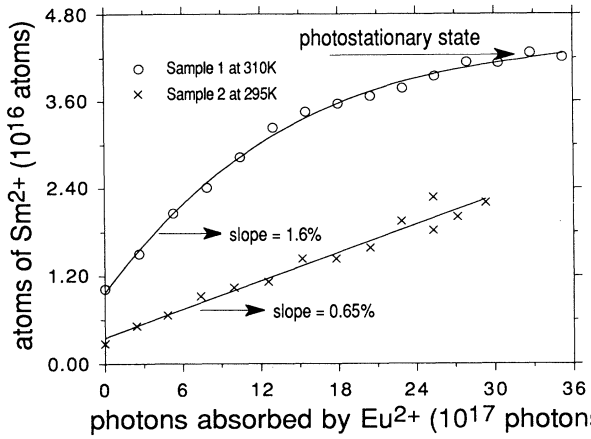

FIG. 4. A plot of the number of divalent samarium atoms formed by irradiation of a SrF_2:0.01 Eu,0.02% Sm crystal vs the total number of 4.9-eV photons absorbed by divalent europium at room temperature. The slope of this curve corresponds to the ionization efficiency of Eu^{2+} in SrF_2 which has been calculated to be 1.6% at 310 K and 0.65% at 295 K. At longer irradiation times, sample 1 achieved a photostationary state implying an ionization efficiency of Sm^{2+} at 310 K and 4.9 eV of 3.4%.

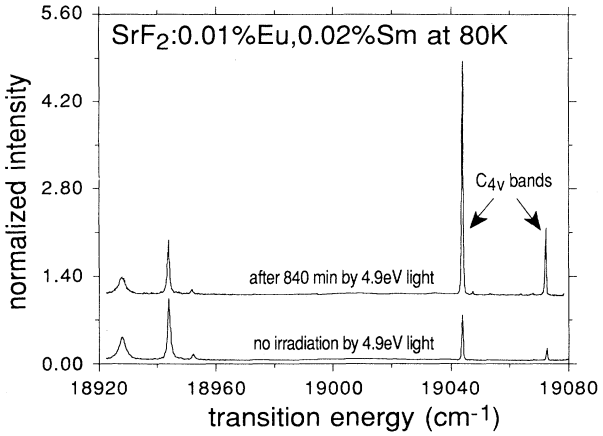

FIG. 5. Two excitation spectra of SrF_2:0.01% Eu,0.02 Sm recorded at 80 K before and after 4.9-eV irradiation at 295 K corresponding to the two states in Fig. 3. The band at 18 944 cm^{-1} is part of the $^6H_{5/2} \rightarrow {}^4F_{3/2}$ transition of Sm^{3+} and the two bands at 19 044 cm^{-1} and 19 077 cm^{-1} are the $^7F_0 \rightarrow {}^5D_1$ transition of $Eu^{3+}\cdot F^-(C_{4v})$. The two strongest bands are shown at their correct energies, but the weaker bands are slightly off since an accurate wave-number calibration was not needed here (also Figs. 6 and 7).

Another feature of Fig. 4 is the reduction of the slope after long exposures. At 4.9 eV, there is an absorption band of Sm^{2+} [the values of $K(Eu^{2+})$ and $K(Sm^{2+})$ are 2.7 and 3.5 cm^{-1} per 0.01% mol at 295 K], and a photostationary state was achieved by the time 36×10^{17} photons were absorbed. Φ_{Sm} was calculated to be 3.4±0.2 % at 310 K and 4.9 eV, assuming $\Phi_{Eu}=1.6\%$.

C. Absolute ionization efficiencies—excitation spectra

Since the Eu^{2+} is in a cubic environment before ionization, we would like to know whether it retains this coordination afterwards, or if it acquires a fluoride compensator. Therefore, we measured the excitation spectra of Sm^{3+} and Eu^{3+} using a narrow (0.5 cm^{-1}) laser line. The Eu^{3+} centers have an absorption, due to the $^7F_0 \rightarrow {}^5D_1$ transition, centered at 19 050 cm^{-1} and they fluoresce at ~17 900 cm^{-1} as well as at other wavelengths.[22] The Sm^{3+} centers absorb at 18 950 cm^{-1} due to the $^6H_{5/2} \rightarrow {}^4F_{3/2}$ transition and also fluoresce at ~17 900 cm^{-1}.[23] Since both of these transitions are close in energy and fluoresce at approximately the same energies, they are ideal for a comparative excitation experiment. Figure 5 shows typical excitation profiles at two states. Because an absolute excitation experiment is extremely difficult to perform, the relative intensities of the bands have been normalized in Fig. 5 so that the largest 19 044-cm^{-1} band of the Eu^{3+} absorption reflects the amount of Eu^{2+} destroyed by the photoionization process and, hence, the amount of Eu^{3+} formed. After this normalization, it is apparent that the bands for the Sm^{3+} do not change in intensity. This result is expected since the large excess of Sm^{3+} present in the crystal, 4×10^{18} atoms/cm^3, is much greater than the small amount of Sm^{2+} formed, typically 1×10^{17} atoms/cm^3 at the longest irradiation times.

The $^5D_1$ state of Eu^{3+} is probed in the excitation experiment, and from this state information is obtained concerning the symmetry of the Eu^{3+} centers. Zakharchenya *et al.*[24,25] have characterized symmetries of various Eu^{3+} sites in CaF_2 through polarization and stress experiments. Hamers, Wielfeldt, and Wright have also characterized the same system using concentration and crystal-field arguments.[22] Almost all of the Eu^{3+} formed in these experiments at 295 K can be assigned to the tetragonal $Eu^{3+}\cdot F^-$ site; however, a small amount of the cubic and trigonal sites are also formed. The assignment of the tetragonal $Eu^{3+}\cdot F^-(C_{4v})$ site is definite for the SrF_2:Eu^{3+} system; the two sharp bands in Fig. 5 have the ratio of 3:1 which is identical to the ratio reported by Hamers for the CaF_2:$Eu^{3+}\cdot F^-(C_{4v})$ center. The cubic band is 3 cm^{-1} higher in energy and has been assigned from the experiments in Sec. III D. In that subsection, we show that cubic Eu^{3+} centers are formed exclusively upon photoionization at lower temperatures. The other small band which is 3 cm^{-1} lower in energy than the large 19 044-cm^{-1} band has been tentatively assigned to the trigonal defect center. The crystal field for a trigonal center would not split the $^5D_1$ state; hence only one band should be present in absorption. Ionic thermocurrent experiments suggest that in the SrF_2:Gd^{3+} system the interstitial fluorine compensates the Gd^{3+} in both a nearest-neighbor site (C_{4v}) and a next-nearest-neighbor site (C_{3v}).[26] Since the mode of charge compensation depends primarily on the size of the trivalent ion, one could easily argue that Eu^{3+}, a neighbor of the Gd^{3+} in the periodic table, would also have some trigonal $Eu^{3+}\cdot F^-$ centers present. Based on this observation, the unobserved split-

ting, and a lack of a better assignment for the small band at 19 041 cm^{-1}, we assign this band to the trigonal $Eu^{3+}\cdot F^{-}(C_{3v})$ center.

D. Relative ionization efficiencies—low-temperature irradiation

Irradiation of doubly doped samples of SrF_2:Eu,Sm at room temperature was shown to yield only the $Eu^{3+}\cdot F^{-}(C_{4v})$ species as the protoproduct of an initially cubic Eu^{2+}. The observation of $Eu^{3+}\cdot F^{-}(C_{4v})$ centers suggests that the interstitial fluorines can diffuse at room temperature. To prove this concept, the doubly doped SrF_2:Eu,Sm sample was irradiated at room temperature and rapidly quenched before the F_i^{-} could diffuse. Intense 5.2-eV laser light was used to excite the sample. This light is strongly absorbed by the $f^6d(t_{2g})$ state of Eu^{2+}, the same state which the 4.9-eV mercury lamp had irradiated.

The lower spectrum in Fig. 6 is of the SrF_2:Eu,Sm crystal before any ionizing radiation had been absorbed by the sample. Clearly, there is no Eu^{3+} of any form present in the crystal. After ~500 pulses of the 5.2-eV light were allowed to irradiate the sample, a significant amount of the divalent europium was converted to the trivalent state. The crystal was then rapidly quenched to 80 K; to be more precise, the thermocouple took only 5 min to reach 80 K. To ensure that the crystal was at 80 K, at least 15 min passed before the excitation scan was begun. The middle spectrum of Fig. 5 shows the excitation profile for this "quenched" crystal. In that spectrum, the peak due to the $Eu^{3+}(O_h)$ center is much more intense than the same band found in the excitation scans in which the crystal had been irradiated with a mercury lamp and remained at room temperature for an extended period of time. The same "quenched" crystal was then warmed back to 300 K and remained at that temperature for over one hour. The excitation spectrum of the annealed crystal is the upper spectrum in Fig. 6, and is identical to those irradiated with the mercury lamp.

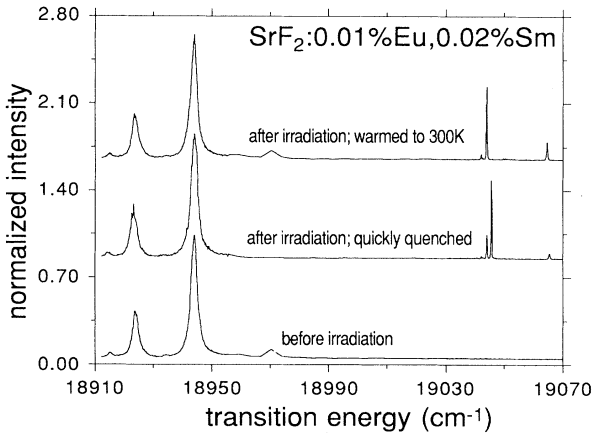

FIG. 6. Excitation spectra before and after ionization of a SrF_2:Eu,Sm sample at 295 K. The lower spectrum shows that no Eu^{3+} is present initially. The middle spectrum records the sample after ionization at 5.2 eV and rapid quenching to 80 K. The majority of the Eu^{3+} formed is cubic; as shown by the presence of the $Eu^{3+}(O_h)$ band at 19 047 cm^{-1}. The upper spectrum records the sample after it had been annealed at 300 K; almost all of the Eu^{3+} is present as $Eu^{3+}\cdot F^{-}(C_{4v})$, showing the strong 19 044 cm^{-1} band.

The three spectra in Fig. 6 have all been normalized so that the amount of Sm^{3+} remains constant. For accurate comparisons between two excitation scans, one must make sure that the experimental conditions are nearly identical. Because the quantum efficiency of fluorescence varies greatly with temperature for both the SrF_2:Eu^{3+} and the SrF_2:Sm^{3+} systems, the crystal temperature was always maintained at exactly 80 K in the excitation scans.

By comparing the ratios of the Eu^{3+} to Sm^{3+} peaks in Fig. 6 to the ratios observed in the mercury lamp experiment, the total amount of ionization at 5.2 eV was established. A measurement of the laser power per pulse times the number of pulses gave the number of incident photons, nearly all of which were absorbed. The ionization efficiency found this way was roughly 1% at 295 K. The absolute accuracy of this measurement is not as high as in the mercury lamp experiment, but in this case we were interested primarily in the *relative* ionization efficiency of Eu^{2+} measured at different temperatures.

The spectral properties of the cubic Eu^{3+} center and the tetragonal Eu^{3+} center are very similar. Their lifetimes are both approximately 8 ms and they both fluoresce at the same wavelength within the resolution of the monochrometer (4 nm or 125 cm^{-1}). These properties indicate that the F_i^{-} causes only a slight perturbation of the center. Upon converting $Eu^{3+}(O_h)$ into $Eu^{3+}\cdot F^{-}(C_{4v})$ by annealing, we found that the total absorption strength of the $Eu^{3+}\cdot F^{-}(C_{4v})$ bands equals that of the $Eu^{3+}(O_h)$ bands. This is a further demonstration that the interstitial fluorine merely splits the energy level but does not otherwise affect the wave functions.

E. Relative ionization efficiency versus temperature

The diffusion of the interstitial fluorines at room temperature in the doubly doped SrF_2:Eu,Sm crystals permitted a relative efficiency experiment to be performed in the following manner. First, a crystal was irradiated for a short time with 5.2-eV light at 295 K and subsequently remained at that temperature until all of the trivalent europium which had been formed was in the tetragonal form. An excitation scan recorded the spectrum of this annealed state. Then the sample was cooled to a desired temperature and was subsequently ionized with the 5.2-eV light. An excitation scan recorded this spectrum which is expected to be a composite of the $Eu^{3+}\cdot F^{-}(C_{4v})$ centers from the initial ionization at 295 K and the cubic Eu^{3+} centers from the ionization at the lower temperature.

In Fig. 7, two typical spectra are shown. In these spectra, the ratio of the largest $Eu^{3+}\cdot F^{-}(C_{4v})$ peak to the largest $Sm^{3+}\cdot F^{-}(C_{4v})$ peak is the same for both treatments, indicating that no fluorines are diffusing at 200 K (the temperature of the second irradiation period). The height of the $Eu^{3+}(O_h)$ peak can be compared to that of the large $Eu^{3+}\cdot F^{-}(C_{4v})$ peak which was formed by irra-

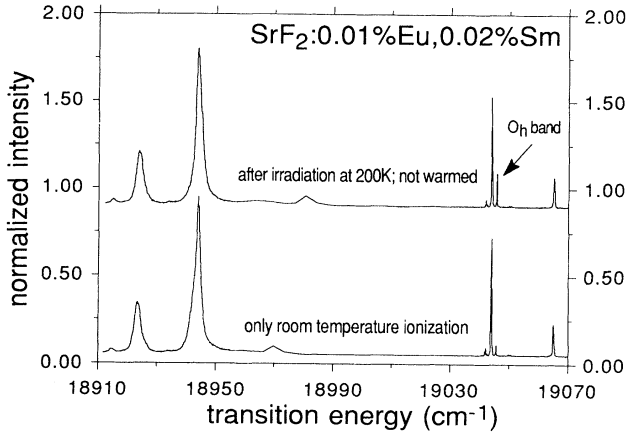

FIG. 7. Typical excitation spectra used in the relative efficiency experiment. The lower spectrum records the SrF_2:Eu,Sm crystal after it had been irradiated at 5.2 eV and subsequently annealed to form $Eu^{3+}\cdot F(C_{4v})$. The upper spectrum records the sample after it had been irradiated at 200 K. The sample was not warmed so that all of the Eu^{3+} formed was cubic (O_h).

diation at 295 K. The ratio of these two bands is directly proportional to the relative efficiency of Eu^{3+} formation at 200 K. Repeating this procedure at different temperatures, the plot shown in Fig. 8 was obtained. At temperatures greater than 220 K, some of the Eu^{3+} was converted into the $Eu^{3+}\cdot F^-(C_{4v})$ species; this conclusion was drawn because an increase in the ratio of the largest $Eu^{3+}\cdot F^-(C_{4v})$ peak to the largest $Sm^{3+}\cdot F^-(C_{4v})$ peak was observed. However, by carefully measuring these intensities, the net amount of Eu^{3+} formed could be calculated. The plot in Fig. 8 clearly contains two regions, the region below 200 K that is insensitive to temperature and the region above 200 K which reflects some activated process. The slope of the latter region corresponds to an activation barrier of 0.32±0.02 eV. The 0.02-eV error corresponds to the standard deviation of the least-squares fit.

To investigate the effect of the incident light energy on the temperature dependence of the ionization efficiency, an experiment which was identical to the previous one was performed, except that light from the second anti-Stokes shift at 5.7 eV, instead of the first anti-Stokes shift at 5.2 eV, was used to ionize the sample. The 5.7-eV light is strongly absorbed by the $f^6d(t_{2g})$ state of Eu^{2+}—the same state excited by the 4.9-eV and 5.2-eV light. Using the same methods as in Sec. III D, an estimate of the absolute ionization efficiency was 8±3 % at 295 K. This efficiency represents an order of magnitude increase over the 4.9-eV irradiation.

A plot of the ionization efficiency at 5.7 eV versus temperature is shown in Fig. 9. This plot is remarkably similar to the plot of the ionization efficiency at 5.2 eV versus temperature which is shown in Fig. 8; there is an activated process with a barrier of 0.41±0.02 eV above 200 K and a temperature-insensitive region below 200 K. The least-squares fit of the data below 200 K reveals a slight slope. A direct comparison between the entire ionization efficiency plots at both 5.2 and 5.7 eV implies that the small differences in the slopes could be attributed to scatter in the low number of data points. The difference in the two activation energies above 200 K could therefore be attributed to random errors, but there is a possibility that they are actually different. By using the data from both of the 5.2- and 5.7-eV experiments, the fit of the activation barrier above 200 K is recalculated to be 0.34±0.04 eV. Because there is little difference between these two plots, the temperature dependence is likely to be determined not by the ionization process, but by the trapping and recombination processes.

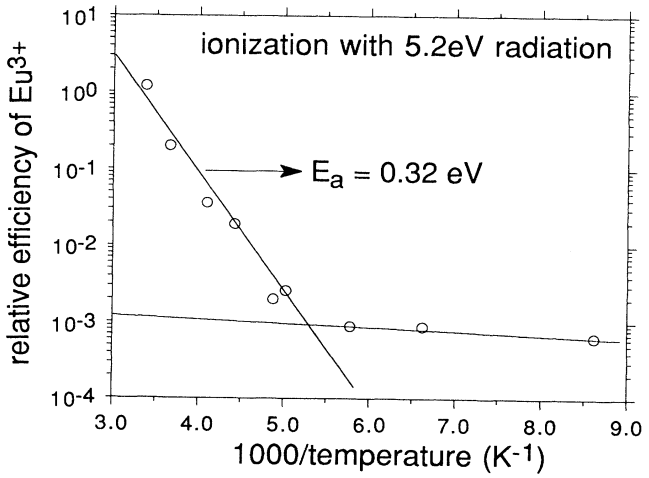

FIG. 8. A plot of the relative efficiency of Eu^{3+} formation at 5.2 eV vs the inverse of temperature. The plot is constructed from the data such as that in Fig. 7. The slope of the line fitted to the high-temperature data yields an activation barrier of 0.32±0.02 eV.

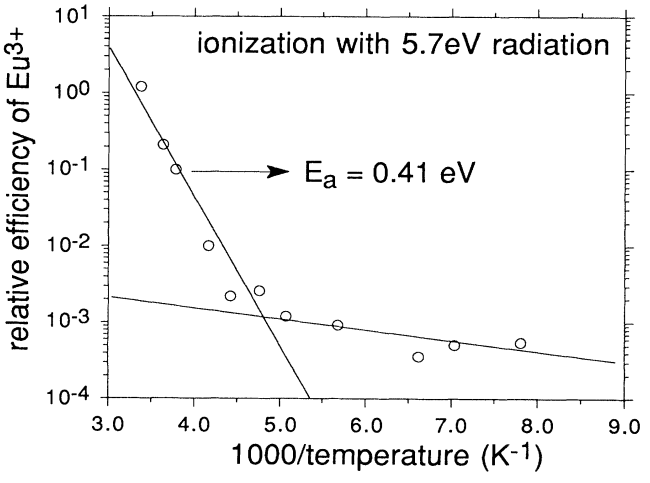

FIG. 9. A plot of the relative efficiency of Eu^{3+} formation at 5.7 eV vs the inverse of temperature. Although the plots in this figure and Fig. 8 are almost identical, the absolute ionization efficiency is about eight times higher here.

IV. DISCUSSION

The result that the ionization yield is a strong function of temperature is very interesting by itself, and also somewhat puzzling when compared to several reports which show that photoconductivity does not vary strongly with temperature.

Photoconductivity measurements at 80 and 295 K were made for SrF_2:0.01% Eu,0.02% Sm in the "initial" state, i.e., before reduction of Sm^{3+} and in the "green" state, after substantial conversion to Sm^{2+} (Figs. 1 and 2). The absolute magnitude of the signal was the same at the two temperatures within a factor of 4 for all wavelengths. While we have not made a more detailed study of the temperature dependence of photoconductivity, there are other reports of a small temperature dependence. Moine, Courtois, and Pedrini reported the photocurrent versus temperature of SrF_2:Yb^{2+} from 100 to 300 K, and showed a maximum variation by a factor of 4 in the range.[27] Pedrini has shown a similar insensitivity to temperature for CaF_2:Tm^{2+} and several others.[28] Anderson in earlier work on photoconductivity of these systems reported that there was no substantial difference between photocurrents at 300 and 80 K.[29] In our measurements on SrF_2:Eu,Sm, there could well be a change in the photocurrent between 80 and 300 K, but it is probably not large.

The magnitude of the photocurrent depends primarily on three factors: the ionization efficiency, the recombination rate, and the trap distances. The ionization efficiency should be independent of temperature because it is a fast process, occurring in a time short compared to the thermal relaxation of the excited ion into the lowest excited state and therefore, less than a few picoseconds. Reported measurements of the line broadening due to photoionization narrow the range further, to the order of 100 fs.[3,4] If the electron is ejected with an excess kinetic energy equal to $h\nu - E_0$, where E_0 is the threshold energy, this energy is usually much greater than kT, hence the electron will be influenced by the strong Coulomb fields of the donor ion and the traps rather than by the phonons before it achieves thermal equilibrium and can diffuse. The Onsager radius is usually greater ($r_c = 86$ Å at 295 K, Ref. 30) than the distance from donor to trap in our samples ($r_{ave} = 59$ Å). Therefore, it seems reasonable that the photoconductivity should be found to be nearly independent of temperature; but then why is the quantum yield strongly dependent on it above 200 K? The quantum yield at 300 K is 10^3 times more than at 200 K, according to Figs. 8 and 9.

Our explanation is that the electrons induce a reverse current of interstitial fluoride (F_i^-) ions going from trap to donor and that this current largely cancels the photocurrent. Below 200 K, there is no significant ion current. The measured activation energy of 0.34 eV for the ionization yield will be shown to be nearly that which is expected for the dissociation of the $Sm^{3+}\cdot F^-$ pairs. The electrons are trapped exclusively by the Sm^{3+} ions, as we showed earlier—no other traps are present in significant amounts compared to the amount of Sm^{3+} added to the crystal. Most of the Sm^{3+} ions are present in the form of $Sm^{3+}\cdot F^-$ pairs; only the small fraction of ions, as determined by thermodynamic equilibrium, are uncompensated because of the large dissociation energy of the $Sm^{3+}\cdot F^-$ complex and because the interstitial fluorines can diffuse easily through the lattice.

In the absolute yield experiments, as much as 14% of the Eu^{2+} ions were converted, far more than could be accounted for if the electrons were trapped at uncompensated Sm^{3+} sites. After the electron is trapped, the interstitial fluorine then moves in the direction of the donor by a series of lattice-interstitial interchanges. The activation energy for the entire process is presumably related to the activation energy for the quantum yield measured in this work.

The value for this process is found to be 0.34±0.04 eV, while the dissociation energy of a $Sm^{3+}\cdot F^-$ complex is $E_d = 0.57$ eV,[26] and the diffusion energy of F_i^- in SrF_2 is $E_a = 0.95$ eV.[31] The 0.34-eV energy is less than either of the other two, and we now speculate on this value.

The activation energy for trapping must certainly involve dissociation of the $Sm^{3+}\cdot F^-$ complex; the following scheme is envisaged:

$$Eu^{2+} \overset{h\nu}{\rightleftarrows} Eu^{3+} + e^- , \tag{2}$$

$$e^- + Sm^{3+}\cdot F^- \rightleftarrows (Sm^{3+} + \cdot F^-)^- \rightarrow Sm^{2+} + F_i^- , \tag{3}$$

$$Eu^{3+} + F_i^- \rightarrow Eu^{3+}\cdot F^- . \tag{4}$$

The energy for Eq. (3) may be less than E_d because the presence of the electron will facilitate the breakup of the complex. After reaction (3) has occurred, the interstitial fluorine then diffuses in the attractive field of the electron donor Eu^{3+} because the retarding Coulomb field of the Sm^{3+} has been canceled. This will explain the yield above 200 K; however, as the temperature is reduced below 200 K, the second step in Eq. (3) becomes slower and the electron can only be trapped at the undissociated $Sm^{3+}\cdot F^-$ complexes, having a small trapping cross section, or at the low number of uncompensated Sm^{3+} sites. Lastly, the wavelength dependence of the ionization yield shown in Figs. 8 and 9 can be explained best as a reduction of the recombination rate due to the greater distance traveled by the electron from the donor ion.

An important question which remains is how far must the electron travel from its donor Eu^{2+} to the trap. In Fig. 4, 4.2×10^{16} Eu^{2+} (in 0.0871 cm^3) were produced by the end of the 310-K run; there are 4.04×10^{18} Sm^{3+}/cm^3 in the sample. Therefore, 14% of the Sm^{3+} ions were reduced to Sm^{2+}. For a random distribution of Eu at $x = 0.0001$ and Sm at $x = 0.0002$ in SrF_2, there is an average of one impurity in every sphere with a 59-Å radius; this corresponds to a length of about ten lattice units. Therefore, in the above experiment the average value of the electron range need not be greater than this in order to explain the results. The Onsager radius in this crystal is 86 Å at 300 K and 130 Å at 200 K, so the traps are generally at a shorter distance; i.e., the Coulomb fields are important at the distances involved in electron trapping and in fluoride migration as we assumed in the preceding paragraph.

The photoconductivity measurements illustrated in Fig. 1 show that the thresholds for photoionization of Eu^{2+} and Sm^{2+} are about 4.7 eV (38 100 cm^{-1}) and 3.4 eV (27 100 cm^{-1}), respectively. Earlier measurements suggest lower values; however, after the samples have been irradiated for a long time, species having lower ionization potentials apparently are formed.[1] A possible species would be Sm^{2+} with a F_i^- compensator nearby, either in the nearest interstitial site or in the nearby trigonal site. In BaF_2:Tm^{2+}, there is evidence for both of these and they are interconvertible by visible light.[32] These higher values for the threshold remove the anomaly mentioned in Ref. 1 for these ions: They are close to the values of 4.45 and 3.06 eV predicted by the electrostatic model.

Finally, we need to elaborate our explanation for the temperature-independent photoconductivity in relation to the results of our yield experiments. Two factors must be considered. Firstly, the number of electrons being measured in a photoconductivity experiment is small compared to the numbers involved in measuring the yields. The currents measured are $\sim 10^{-13}$ A, or 10^6 electrons in the external circuit; this translates into 10^{10} electrons in a 1-mm crystal for a 1000-Å donor to trap distance. This is six orders of magnitude less than the numbers involved in the yield measurements.

Secondly, the photocurrent measurement takes only a few seconds while the yield measurements are taken over hundreds of minutes. We suppose the events registered in a photocurrent experiment are mainly due to electron trapping at the uncompensated Sm^{3+}, whose dipole length may be 1000 Å or more while the contributions due to trapping at the more numerous $Sm^{3+}\cdot F^-$ complexes are lessened because of their smaller dipole and because of the reverse F_i^- current. While the diffusion of interstitial fluorines is slow when dealing with 10^{16} ions, it is fast enough for the 10^{10} electrons in the photocurrent measurement to cancel a large part of the photocurrent, and thus to explain the temperature insensitivity. We are carrying out temperature- and time-dependent photocurrent studies to put these ideas on a firmer basis.

V. CONCLUSION

We have found that the photoionization yield of Eu^{2+} in SrF_2 codoped with Sm^{3+} is dependent on temperature above 200 K with an activation energy of 0.34 eV, and nearly independent of temperature below 200 K. The same temperature dependence was observed at 5.2 eV and 5.7 eV, where the absolute ionization yields were $\sim 1\%$ and $\sim 8\%$, respectively, at 295 K. In more accurate experiments, we found an absolute ionization efficiency of Eu^{2+} in SrF_2 at 4.9 eV of $0.65\pm 0.2\%$ at 295 K and $1.6\pm 0.2\%$ at 310 K. The photocurrent was found to be the same at 80 and 300 K and therefore assumed to be independent of temperature in this range.

These results can be interpreted to show that there are two kinds of electron trapping processes following photoionization; one is the trapping at a $Sm^{3+}\cdot F^-$ complex at distances 50–100 Å from the donor Eu^{2+}, followed by diffusion of interstitial fluorines from trap to donor. The other is trapping at the rare uncompensated Sm^{3+}. Only the latter contributes to the photocurrent.

ACKNOWLEDGMENTS

This work was supported by the Department of Energy, Office of Basic Energy Sciences, under Grant No. DE-FG02-84ER45146.

[1] D. S. McClure and C. Pedrini, Phys. Rev. B **32**, 8465 (1985).
[2] C. Pedrini, F. Rogemond, and D. S. McClure, J. Appl. Phys. **59**, 1196 (1986).
[3] R. L. Fuller and D. S. McClure, J. Lumin. **38**, 193 (1987).
[4] R. L. Fuller and D. S. McClure, J. Lumin. **45**, 354 (1990).
[5] P. P. Feofilov, Opt. Spectrosk. **12**, 531 (1962); **12**, 296 (1962); B. Welber, J. Chem. Phys. **42**, 4262 (1965).
[6] K. Chakrabarti, V. K. Mathur, J. F. Rhodes, and R. J. Abbundi, J. Appl. Phys. **64**, 1363 (1988).
[7] H. von Seggern, T. Voigt, W. Knüpfer, and G. Lange, J. Appl. Phys. **64**, 1405 (1988).
[8] Z. J. Kiss and P. N. Yocum, J. Chem. Phys. **41**, 1511 (1964).
[9] F. K. Fong and M. A. Hiller, J. Phys. Chem. **71**, 2854 (1967).
[10] Optovac, Inc., North Brookfield, MA.
[11] C. Pedrini, D. S. McClure, and C. H. Anderson, J. Chem. Phys. **70**, 4959 (1979).
[12] C. A. Parker, Proc. R. Soc. London **A220**, 104 (1953).
[13] C. G. Hatchard and C. A. Parker, Proc. R. Soc. London Sect. A **235**, 518 (1956).
[14] D. Eimerl, L. Davis, S. Velsko, E. K. Graham, and A. Zalkin, J. Appl. Phys. **62**, 1968 (1987).
[15] R. E. Randeau, J. Chem. Eng. Data **11**, 124 (1966).
[16] R. L. Fuller, Ph.D. thesis, Princeton University, 1990 (unpublished), pp. 146–154.
[17] D. S. McClure and Z. J. Kiss, J. Chem. Phys. **39**, 3251 (1963).
[18] E. Loh, Phys. Rev. **175**, 533 (1968).
[19] H. A. Weakliem, C. H. Anderson, and E. S. Sabisky, Phys. Rev. B **1**, 4354 (1970).
[20] W. Kaiser, C. G. B. Garrett, and D. L. Wood, Phys. Rev. **123**, 766 (1961).
[21] V. Arkhangel'skaya, M. Kiselyeva, and V. Shraiber, Opt. Spektrosk. **23**, 509 (1967) [Opt. Spectrosc. **23**, 275 (1967)].
[22] R. J. Hamers, J. R. Wietfeldt, and J. C. Wright, J. Chem. Phys. **77**, 683 (1982).
[23] N. Rabbiner, J. Opt. Soc. Am. **57**, 1376 (1967).
[24] B. P. Zakharchenya and I. B. Rusanov, Fiz. Tverd. Tela (Leningrad) **8**, 41 (1966) [Sov. Phys. Solid State **8**, 31 (1966)].
[25] B. P. Zakharchenya, I. B. Rusanov, and I. I. Takhistova, Fiz. Tverd. Tela (Leningrad) **8**, 3602 (1966) [Sov. Phys. Solid State **8**, 2877 (1967)].
[26] P. Dorenbos, S. Vrind, J. Dolfing, and H. W. den Hartog, Phys. Rev. B **35**, 5766 (1987).
[27] B. Moine, B. Courtois, and C. Pedrini, J. Lumin. **45**, 248 (1990).
[28] C. Pedrini, F. Gaume-Mahn, and D. S. McClure, in *The Rare Earths in Modern Science and Technology*, edited by G. J. McCarthy, H. B. Silber, and J. J. Rhyne (Plenum, New York, 1982), Vol. 3, p. 165.
[29] C. H. Anderson (unpublished).
[30] L. Onsager, Phys. Rev. **54**, 554 (1938).
[31] W. Bollmann, P. Görlich, W. Hauk, and H. Mothes, Phys. Status Solidi **2**, 157 (1970).
[32] E. S. Sabisky and C. H. Anderson, Phys. Rev. **159**, 234 (1967).